EUROPEAN ORGANIZATION FOR NUCLEAR RESEARCH

CERN-EP/88-92
August 4th, 1988

EVIDENCE OF ISOSPIN EFFECTS IN ANTIPROTON-NUCLEUS ANNIHILATION

F. Balestra, S. Bossolasco, M.P. Bussa, L. Busso, L. Ferrero,
D. Panzieri, G. Piragino and F. Tosello
Istituto di Fisica Generale 'A. Avogadro', University of Turin and
INFN, Sezione di Torino, Turin, Italy

R. Barbieri, G. Bendiscioli, A. Rotondi, P. Salvini, A. Venaglioni and A. Zenoni
Dipartimento di Fisica Nucleare e Teorica, University of Pavia and
INFN, Sezione di Pavia, Italy

Yu. A. Batusov, I.V. Falomkin, G.B. Pontecorvo, A.M. Rozhdestvensky
M.G. Sapozhnikov and V.I. Tretyak
Joint Institute for Nuclear Research, Dubna, USSR

C. Guaraldo and A. Maggiora
Laboratori Nazionali di Frascati dell'INFN, Frascati, Italy

E. Lodi Rizzini
Dipartimento di Automazione Industriale, University of Brescia and
INFN, Sezione di Pavia, Italy

A. Haatuft, A. Halsteinslid, K. Myklebost and J.M. Olsen
Physics Department, University of Bergen, Norway

F.O. Breivik, T. Jacobsen and S.O. Sørensen,
Physics Department, University of Oslo, Norway

ABSTRACT

Antiproton-^{3}He annihilation events at rest have been detected using a self shunted streamer chamber. The ratio of the cross section for annihilation on neutrons and on protons has been measured (0.467 ± 0.035). It is compared with other results from annihilation on free nucleons, deuterium, ^{3}He and ^{4}He. The low value of the ratio seems to indicate a strong isospin dependence of the antinucleon-nucleon P-wave.

(Submitted to Nuclear Physics)

1 *Introduction*

The antiproton-neutron ($\bar{p}n$) system is in a pure isospin state with I=0 and the antiproton-proton ($\bar{p}p$) system is in a mixture of states with I=0 and I=1. If we indicate with $f_I(\theta)$ the spin averaged scattering amplitude for the state with isospin I, for the $\bar{p}n$ and the $\bar{p}p$ systems we have scattering amplitudes:

$$f^{el}_{\bar{p}n}(\theta) = f_1(\theta) \qquad 1.1$$

$$f^{el}_{\bar{p}p}(\theta) = \frac{1}{2}(f_0(\theta) + f_1(\theta)) \qquad 1.2$$

$$f^{ce}_{\bar{p}p}(\theta) = \frac{1}{2}(f_0(\theta) - f_1(\theta)) \qquad 1.3$$

where 'el' means elastic and 'ce' means charge exchange .

The annihilation cross section for the $\bar{p}n$ system is :

$$\sigma^{a}_{\bar{p}n} = \sigma^{t}_{1} - \sigma^{el}_{1} \equiv \sigma^{a}_{1} \qquad 1.4$$

where σ^{t}_{1} means total cross section and σ^{el}_{1} is the total elastic cross section. For the $\bar{p}p$ system the annihilation cross section is given by :

$$\sigma^{a}_{\bar{p}p} = \sigma^{t}_{\bar{p}p} - (\sigma^{el}_{\bar{p}p} + \sigma^{ce}_{\bar{p}p}) = \frac{1}{2}(\sigma^{a}_{0} + \sigma^{a}_{1}) \qquad 1.5$$

where all the quantities are total cross sections.

Hence:

$$R^{a} = \frac{\sigma^{a}_{\bar{p}n}}{\sigma^{a}_{\bar{p}p}} = \frac{2\,\sigma^{a}_{1}}{\sigma^{a}_{0} + \sigma^{a}_{1}} = \frac{2\dfrac{\sigma^{a}_{1}}{\sigma^{a}_{0}}}{1 + \dfrac{\sigma^{a}_{1}}{\sigma^{a}_{0}}} \qquad 1.6$$

and

$$\frac{\sigma_1^a}{\sigma_0^a} = \frac{R^a}{2 - R^a} \qquad 1.7$$

Eq.(1.7) allows the relative intensities of the I=1 and I=0 interactions to be evaluated, when the value of R^a is known experimentally .

We note that if the $\bar{N}N$ interaction is independent of the isospin, i.e. $\sigma^a{}_1/\sigma^a{}_0=1$, $R^a=1$ (and viceversa) (see Fig.1). Consequently, if R^a is found experimentally to be other than 1, it indicates that the $\bar{N}N$ interaction depends on the isospin.

The previous considerations concern annihilation of free nucleons, but in the following we shall consider also annihilation on nucleons bound in mass A nuclei. For this purpose, we define the ratio

$$R_b^a = \frac{\sigma_b^a(\bar{p}n)}{\sigma_b^a(\bar{p}p)} \qquad 1.8$$

where b means bound and $\sigma^a{}_b(\bar{p}n)$ and $\sigma^a{}_b(\bar{p}p)$ are cross sections for annihilation on single nucleons bound in the nucleus.

This paper contributes to the study of the isospin dependence of $\bar{N}N$ annihilation at low energy (below 600 MeV/c) through a review of some existing data on R^a and $R^a{}_b$ (Sect.2), a new measurement of $R^a{}_b$ at rest (on ^{3}He nuclei, Sect.3) and a discussion which shows the different isospin dependences of the S and P $\bar{N}N$ states (sect.4). The main conclusions are summarized in Sect.5.

2 *Experimental situation*

2.1 Data on R^a

Experimental information on R^a comes (a) from antinucleon-nucleon data, (b) from Glauber theory analysis of $\bar{p}$-nucleus elastic scattering and total cross section data and (c) from analysis of $\bar{p}^3$He and $\bar{p}^4$He annihilation events.

(a) There are more sets of data on $\bar{p}p$ annihilation in the interval 300-600 MeV/c [1-7] and only one below 300 MeV/c [8]. Some data are reported in Fig.2. We stress that all the data displayed concern total $\bar{p}p$ annihilation cross sections. Because most of the original papers report cross sections for $\bar{p}p$ annihilation into charged pions or for $\bar{p}p$ inelastic interaction (i.e., annihilation plus $\bar{p}p \rightarrow \bar{n}n$ charge exchange), we have

corrected the data by adding the cross section for annihilation into neutral mesons [2,3,4,5,6] or by subtracting the cross section for the charge exchange interaction [8] . The cross sections for the reaction $\bar{p}p$ ->neutrals (annihilation into neutrals plus charge exchange) are reported in Refs.1,2 and 9 and those for charge exchange in Refs.10-11 (see also Fig.3). The difference between these two quantities gives the cross section for the annihilation with production of neutral mesons . This cross section decreases from about 7 mb down to about 4 mb between 300 and 600 MeV/c, where can be approximately expressed by the formula :

$$\sigma^a_0 \text{(mb)} \simeq 8 - p(\text{MeV/c})/150.$$

The points of Ref.8 are corrected considering the charge exchange data of Ref.12, which differ somewhat from those of Ref.10 below 250 MeV/c.

The lines in Fig.2 were obtained by the formulas :

$$\sigma^a(\bar{p}p) = (36.5 \pm 3.2) + (28.9 \pm 1.7)/p \qquad \text{for } 0.43<p<0.6 \text{ (Lowenstein et al., Ref.4)}$$

$$\sigma^a(\bar{p}p) = (8.5 \pm 2.5) + (40.7 \pm 1.3)/p \qquad \text{for } 0.3<p<0.6 \text{ (Brando et al.,Ref.6)}$$

$$\sigma^a(\bar{p}p) = (29.43 \pm 1.83) + (32.0 \pm 0.92)/p \qquad \text{for } 0.42<p<0.6 \text{ (Brueckner et al.,Ref.7)}$$

$$\sigma^a(\bar{p}p) = (-3.6 \pm 5.8) + (44.1 \pm 2.7)/p \qquad \text{for } 0.375<p<0.7 \text{ (Sai et al., Ref.5)}$$

where σ^a is in mb and p in GeV/c. They are corrected for σ^a_0.

The figure shows that above 400 MeV/c the data of Chaloupka et al. and Lowenstein et al. have the same behaviour; the same holds for those of Brueckner et al. [3] and of Brando et al.

It is remarkable that the line of Brando et al., which was obtained by fitting data above 300 MeV/c, agrees very well also with the data of Brueckner et al. [8], when it is extrapolated down to 175 MeV/c. The same tendency is shown also by new annihilation data below 440 MeV/c obtained by the latter authors [13].

Summarizing, above 400 MeV/c the data are spread and below that they are poor.

In Fig.2, the line fitting the $\bar{n}p$ data from Ref. 14 is also reported. It is given by the equation :

$$\sigma^a(\bar{n}p) = (41.4 \pm 9.0) + (29.0 \pm 2.9)/p$$

where σ^a is in mb and p in GeV/c.

In the figure the statistical errors on the $\bar{n}p$ data are indicated ; the systematic errors are of the same order of magnitude. The $\bar{n}p$ line is superimposed on the pp line of Lowenstein et al. above 400 MeV/c.

Considering the large errors (both systematic and statistical), the figure suggests $\sigma^a(\bar{n}p) < \sigma^a(\bar{p}p)$ below 400MeV/c and $\sigma^a(\bar{n}p) \simeq \sigma^a(\bar{p}p)$ above, but with a large degree of uncertainty.

(b) Kondratyuk and Sapozhnikov [15] analyzed, in the framework of the Glauber theory, experimental data on the total cross sections of antiproton-deuterium scattering in the interval 200-800 MeV/c, in order to evaluate the antiproton-neutron total and annihilation cross sections. They found different sets of results corresponding to different experimental data on the total antiproton-deuteron cross section. To probe the reliability of the different sets, they calculated the reaction cross sections for the antiproton-nucleus scattering and found the best agreement with the experimental data with the formulas :

$$\sigma^t(\bar{p}n) = 65.52 + 38.09/p$$

$$\sigma^a(\bar{p}n) = 36.22 + 25.05/p$$

This value of $\sigma^a(\bar{p}n)$ is lower than that of Armstrong et al. for $\bar{n}p$ annihilation. Divided by the $\sigma^a(\bar{p}p)$ values of Brando et al., it gives a ratio R^a which increases from about 0.7 at 200 MeV/c up to about 1 at 600 MeV/c. Of course, the values of R^a are affected by the uncertaines on $\sigma^a(\bar{p}p)$ seen previously and by those on the $\bar{p}p$ scattering parameters assumed as input data of the Glauber calculation.

(c) Annihilation events at rest on ^{3}He and ^{4}He are analyzed, through an approximated procedure, in Ref.16. Fits to the π^- multiplicity distributions having R^a as a free parameter lead to $R^a = 0.35 \pm 0.07$ for ^{3}He and $R^a = 0.48 \pm 0.10$ for ^{4}He. These values show that the $\bar{N}N$ interaction depends strongly on the isospin ($\sigma^a_1/\sigma^a_0 = 0.21$ and 0.31, respectively).

2.2 *Data on R^a_b*

The $\bar{p}^2H$ annihilation below 600 MeV/c is studied in bubble chambers [17,18]. The annihilation events are separated into two sets: events with features of annihilations on n (with an odd number of charged pions) and events with features of annihilations on p (with an even number of charged pions). The ratio between the two numbers of events gives the values of R^a_b and has the behaviour shown in Fig.4. It is near constant and equal to $\simeq 0.8$. Note that annihilations at rest include annihilations with antiproton momentum less than approximatively 300 MeV/c.

With a procedure similar to that utilized in the ^2H case, although more cumbersome, the ratio R^a_b is also obtained from $\bar{p}^4He$ annihilation data [19,20]. The values are reported in Fig.4. At rest and at 600 MeV/c, they are sensibly lower than the values obtained from deuterium. Above 200 MeV/c, this is due in part to some small approximation in the analysis of the events (for instance, concerning $\bar{p}p \to \bar{n}n$ charge exchange effects; see Ref.19). Note that the ratio R^a_b is not affected by systematic errors on the cross sections similar to those affecting the data considered in Sect.2.1 (a) and (b). Indeed, in the present analyses, the values of R^a_b are carried out by means of cross section values obtained in the same experiment; so effects dependent on different normalizations are avoided. The same comment holds for the analysis mentioned in Sec.2.1 (c).

The above review shows that the annihilation process depends on the isospin state of the antinucleon-nucleon system. Because R^a and R^a_b are smaller than 1, the I=0 interaction is stronger than the I=1 one (see eq.1.7).

3 *Measurement of R^a_b at rest on ^3He*

3.1 *$\bar{p}$ ^3He annihilation*

In a conventional picture, the annihilation process of $\bar{p}$ on ^3He nuclei at rest consist of a $\bar{p}$-nucleon annihilation which may be followed by the interaction between the residual nucleons and the pions produced by the annihilation (final state interaction, FSI). Here we neglect the production of strange particles, which occurs in a few percent of the cases and is unimportant to the following .

If only annihilation is effective and FSI is not , $\bar{p}p$ annihilation produces an even number of charged pions and a ^2H nucleus ; $\bar{p}n$ annihilation produces an odd number of charged pions and two protons. Hence, the annihilation processes on n and on p are distinguishable both by the number of charged pions and by the number of heavy prongs. In any case , all events have an odd number of charged prongs.

FSI may break the ^2H nucleus or, through the π-nucleon charge exchange reactions ($\pi^- p \leftrightarrow \pi^\circ n$, $\pi^\circ p \leftrightarrow \pi^+ n$) may change the primary number of charged pions

and charged heavy prongs. An important consequence of the charge exchange is that the $\bar{p}p$ annihilation events may assume the features of events due to $\bar{p}n$ annihilations and viceversa, as it affects the relative number of heavy and light particles emitted. This fact is illustrated by the examples in Tab.1. We see that, in general, there is no distinction between events due to $\bar{p}n$ and $\bar{p}p$ annihilation on the basis of the number of heavy and light particles. Nevertheless, it is possible to evaluate the ratio between the probabilities of annihilation on n and on p , as we show in the next section, following the procedure described in more detail in Ref.19. This procedure is based on the distinction between π and heavier particles among the final product of the reactions.

3.2 *Evaluation of* R^a_b

Experimentally, we can divide the events into two sets (a) and (b). (a) includes (i) direct $\bar{p}p$ annihilations; (ii) $\bar{p}p$ annihilations plus FSI without final charge exchange on n ($\pi^0 n, \pi^+ n$); (iii) $\bar{p}n$ annihilations plus final charge exchange on p ($\pi^0 p, \pi^+ p$). Set (a) includes mostly $\bar{p}p$ annihilations and $\bar{p}n$ annihilations which look like $\bar{p}p$ annihilations due to pion charge exchange. (b) includes (i) direct $\bar{p}n$ annihilations; (ii) $\bar{p}n$ annihilations plus FSI without final charge exchange on p ($\pi^0 p, \pi^+ p$);(iii) $\bar{p}p$ annihilations plus FSI final charge exchange on n ($\pi^+ n, \pi^0 n$). Set (b) includes mostly $\bar{p}n$ annihilations and $\bar{p}p$ annihilations that look like $\bar{p}n$ annihilations due to the pion charge exchange.

The events belonging to the two sets can be recognized by the number of heavy prongs and the equality of the numbers of π^+ and π^-, as is summarized in Table 2. Of course, all the events with one prong belong to set (a), while the events with a higher multiplicity may belong either to set (a) or to set (b).

We define : $\sigma_m(\bar{p}p)$=cross section for (a) event production; $\sigma_m(\bar{p}n)$=cross section for (b) event production; $\sigma^a(\bar{p}p)$=cross section for annihilation on one p; $\sigma^a(\bar{p}n)$ =cross section for annihilation on one n; $\sigma^p_{ce}(\bar{p}n)$=cross section for annihilation on n plus final charge exchange on p; $\sigma^n_{ce}(\bar{p}p)$=cross section for annihilation on p plus final charge exchange on n; σ^a_t=total annihilation cross section.

$\sigma_m(\bar{p}p)$ and $\sigma_m(\bar{p}n)$ are measured in the present analysis. $\sigma^p_{ce}(\bar{p}n)$ and $\sigma^n_{ce}(\bar{p}p)$ are unknown and should be obtained from the event analysis. However their contribution is negligible (see later on). $\sigma^a(\bar{p}p)$ and $\sigma^a(\bar{p}n)$ are annihilation cross sections on nucleons bound in ^{3}He.

By definition, the following relations hold:

$$2\sigma^a(\bar{p}p) = \sigma_m(\bar{p}p) + \sigma^n_{ce}(\bar{p}p) - 2\sigma^p_{ce}(\bar{p}n) = \sigma_m(\bar{p}p) - \sigma_{ce} \qquad 3.1$$

$$\sigma^a(\bar{p}n) = \sigma_m(\bar{p}n) + 2\sigma^p_{ce}(\bar{p}n) - \sigma^n_{ce}(\bar{p}p) = \sigma_m(\bar{p}n) + \sigma_{ce} \qquad 3.2$$

$$\sigma^a_m(\bar{p}p) + \sigma^a_m(\bar{p}n) = \sigma^a_t \qquad 3.3$$

where

$$\sigma_{ce} = 2\sigma^p_{ce}(\bar{p}n) - \sigma^n_{ce}(\bar{p}p) \qquad 3.4$$

contains terms which tend to cancel each other ($\pi^0 p <=> \pi^+ n$; $\pi^- p <=> \pi^0 n$) .

The factor 2 in front of $\sigma^a(\bar{p}p)$ in eqs.(3.1) accounts for the 2 protons in ^{3}He and that in front of $\sigma^p_{ce}(\bar{p}n)$ accounts for the 2 protons in the final state after annihilation on n.

Having set

$$r = \frac{\sigma_m(\bar{p}n)}{\sigma_m(\bar{p}p)} \qquad 3.5$$

from eqs.(2.1),(2.2) and (2.3) one obtains

$$R^a_b = \frac{\sigma^a(\bar{p}n)}{\sigma^a(\bar{p}p)} = 2\,\frac{r + (r+1)\dfrac{\sigma_{ce}}{\sigma^a_t}}{1 - (r+1)\dfrac{\sigma_{ce}}{\sigma^a_t}} \qquad 3.6$$

Since

$$\sigma_{ce} / \sigma^a_t << 1$$

as it is shown in Ref.16 and19, one obtains the simplified formula:

$$R^a_b = 2\,r \qquad 3.7$$

3.3 *Experimental data analysis*

Events were detected using a self-shunted streamer chamber (90x70x18 cm^3) in a magnetic field (0.4 T) exposed to an antiproton beam (105 MeV/c) from the LEAR

facility of CERN. The apparatus is described in detail in Ref. 21. Some features of the annihilation at rest are reported in Ref.16. One should note the following points. (i) The events are recorded on two cameras with one event per picture. (ii) The beam momentum at the entrance of the chamber is distributed around 70 MeV/c and, consequently, the vertices of the events are spread over a central region ($\sim$ 35 cm long) of the chamber (which is 90 cm in length). (iii) Approximately 85% of annihilations occur with an antiproton momentum of less than 10 MeV/c and the remainder have less than 50 MeV/c. (iv) The gaseus target (at normal conditions of temperature and pressure) allows to detect carefully very slow particles as well as minimum ionization particles.

2020 events have been measured following the procedure described in Ref.22 and 962 events with 3, 5 and 7 prongs have been identified as belonging to set (a) or to set (b). We recall that the one prong events belong only to the set (a) and are 4.90% of the odd prong events (see Tab.3).

Identification of the events is limited as in some cases the masses of the prongs cannot be identified, which depends on the direction of the tracks in relation to the magnetic field direction and on the ionization. Identification is easier for events with a lower number of prongs. Following Ref.19, to overcome this inconvenience, we normalize the identified events with multiplicity i to the percentage of all detected events with the same multiplicity (see Tab.3).

The ratio r is given simply by the ratio between the percentage of events of type (a) and of type (b), reported in Tab.3. In the approximation of Eq.3.7 we obtain (due to the approximation, R^a_b is underestimated by less than 3%):

$$R^a_b = 2r = 2\ (18.93/81.07) = 0.467 \pm 0.035$$

This value is equal to that found in a preceding work for ^{4}He (see Fig.1).

To check our procedure, we calculate the multiplicity distributions of π^- produced in the $\bar{p}p$ and $\bar{p}n$ annihilation events separately and compare them to similar distributions obtained with hydrogen and deuterium in bubble chambers. As shown in Tab.4, the agreement is very good.

4. *Comments*

In this section we comment on the different behaviours of R^a_b from deuterium and from helium, in a particular way at rest.

As seen in Tab.5, the values of R^a_b from the antiproton annihilation at rest on ^{3}He and ^{4}He is twice as large as the corresponding values found in deuterium.

It is useful to compare the experimental values of R^a_b in Tab.5, with predictions of

different theoretical models. In the limit k —> 0, the ratio R^a is connected with the $\bar{N}N$ scattering lengths a_0 and a_1 in S-wave :

$$R^a_S = \frac{2\,\mathrm{Im}\,a_1}{\mathrm{Im}\,a_1 + \mathrm{Im}\,a_0} \qquad 4.1$$

In Tab.6 the values of R^a_S from theoretical models and some experiments are collected. Both theoretical and experimental results show that a large R^a value is in obvious disagreement with the results on He, but in agreement with the results from ^{2}H. The reason is that the annihilation strength depends on the relative motion of the interacting antiproton and nucleon. The relative motion depends on the atomic states from which the antiproton annihilates and on the motion of the nucleon inside the nucleus (that is, on the nucleus structure; for annihilation on ^{2}H, see [28]).

As it concerns the atomic states, cascade model calculations [29] show that the annihilation probability from S-levels in helium gas at 1 atm is only 8%, compared with 49% from P-states and 43% from D-states. On the contrary, in liquid hydrogen the annihilation at rest proceeds mainly from highly excited S-states due to a strong Stark effect [30]. So, it is impossible to directly compare the results from helium gas with those from liquid deuterium, as they refer to different mixtures of $\bar{N}N$ partial waves.

Nevertheless, the differences between the helium and deuterium data can be regarded as an indication of a strong isospin dependence of $\bar{N}N$ -amplitude in P- and/or D-states. In fact, the fits of low-energy $\bar{p}p$ and $\bar{p}n$ data in the effective range approximation for the $\bar{N}N$ -amplitude have shown a substantial isospin dependence in the P-states [31,32]. The analog of the eq(4.1) for the P-wave annihilation is

$$R^a_p = \frac{2\,\mathrm{Im}\,b_1}{\mathrm{Im}\,b_1 + \mathrm{Im}\,b_0} \qquad 4.2$$

where Im b_1 and Im b_0 stand for the imaginary parts of the scattering volumes in the isospin states I=1 and I=0. Mahalanabis et al. [31] fit experimental data on $\bar{p}p$ and $\bar{n}p$ total and differential cross sections below 300 MeV/c and on energy shift and width of antiprotonic hydrogen and find $R^a_p = 0.2$. Grach et al. [32] fit $\bar{p}p$ data at 181 MeV/c obtaining $R^a_p = 0.35$. Grach et al. fit also higher energy data and include D-wave, but their results are contraddictory and further investigations are in progress.

So, the higher R^a_b value in liquid deuterium at rest seems to indicate that S-state prevails, while the lower value in gaseus ^{3,4}He seems to indicate that P and presumably

D-waves prevail.

A similar situation occurs in the annihilation in flight. At the same laboratory $\bar{p}$ momentum, different mixtures of $\bar{N}N$ partial waves are involved in the annihilation on ^2H and on He, so that, in principle,different behaviours of R^a_b must be expected.

An estimation of the contributions of different partial waves to the annihilation cross section is reported in Ref.33. At about 225 MeV/c there are equal contributions from S and P-waves. As the momentum increases, P and D-waves become more and more important.

Both R^a and R^a_b are $<$ 1 between 0 and 600 MeV/c, i.e. $\sigma^a(\bar{p}n) < \sigma^a(\bar{p}p)$.In the present framework of $\bar{N}N$ potentials, this may be a manifestation of a strong actractive central potential in the I=0 state due to coherence of σ and ω exchange terms [34] and to the dependence of the immaginary potential on isospin [26].

5. Conclusions

We can summarized the analyses of the previous sections as follows: measurements of both R^a (free nucleons) and R^a_b (bound nucleons) indicate that below 600 MeV/c these ratios are $\lesssim$ 1 and increase for $\bar{p}$ momenta from 0 up to 600 MeV/c. That is, they show that $\bar{N}N$ annihilation is isospin dependent, particularly at rest on ^3He and ^4He.

At present, the behaviour of the ratio from annihilations on free nucleons is somewhat uncertain, due to normalization problems in the cross sections. A clear indication of the dependence on isospin is given by the annihilation on nuclei.

The different values of R^a_b from ^2H and $^{3,4}He$ are compatible with analyses of $\bar{N}N$ scattering and antiprotonic hydrogen data and indicate that the isospin dependence is stronger in P state than in S state.

Finally, the values of $R^a_b<1$ indicate that the interaction in the isospin state with I=1 is weaker than in the state with I=0.

Aknowledgments

The authors are grateful to T.A.Shibata for useful comments while preparing this paper.

Thanks are due to Mr.Claudio Casella (Pavia) for his highly valuable scanning and measuring work.

REFERENCES

1 - U.Amaldi et al.,Nuovo Cimento 46A(1966)171
2 - V.Chaloupka et al., Phys.Lett.61B(1976)487
3 - W.Brueckner et al.,Phys.Lett.67B(1977)222
4 - D.I.Lowenstein et al.,Phys.Rev.D23(1981)2788
5 - F.Sai et al., Nucl.Phys.B213(1983)371
6 - T.Brando et al.,Phys.Lett.158B(1985)505
7 - W.Brueckner et al., Phys.Lett.B197(1987)463
8 - W.Brueckner et al.,Phys.Lett.B166(1986)113
9 - M.Alston-Garnjost,Phys.Rev.Lett.35(1975)1685
10 - R.P.Hamilton et al.,Phys.Rev.Lett.44(1980)1182
11 - K.Nakamura et al.,Phys.Rev.Lett.53(1984)885
12 - W.Brueckner et al.,Phys.Lett.169B(1986)302
13 - T.A.Shibata, Private communication
14 - T.Armstrong et al., Phys.Rev.D36(1987)659
15 - L.A.Kondratyuk and M.G.Sapozhnikov,
Sov.J.Nucl.Phys.46(1987)56
16 - F.Balestra et al., Nucl.Phys.A474(1987)651
17 - R.Bizzarri et al.,Nuovo Cimento A22(1974)225
18 - T.E.Kalogeropoulos et al.,Phys.Rev.D22(1980)2585
19 - F.Balestra et al., Nucl.Phys.A465(1987)714
20 - F.Balestra et al.,CERN-EP/87-213(1987),In press in Nuovo Cimento
21 - F.Balestra et al., Nucl.Instr.and Meth.A234(1985)30
22 - F.Balestra et al.,Nucl.Instr.and Meth.A257(1987)114
23 - T. Ueda, Prog.Theor.Phys., 62(1979)1670
24 - R.A.Bryan and R.Phillips, Nucl.Phys.B5(1968)201
25 - C.Dover and J.M.Richard, Phys.Rev.C21(1980)1466
26 - J.Coté et al., Phys.Rev.Lett.48(1982)1319
27 - L.Pinsky, Proc.IV LEAR Workshop, Villars(1987)255
28 - R.Bizzarri et al.,Nucl.Phys.B69(1974)298
29 - F.Reifenroether et al., Phys.Lett.B203(1988)9
30 - T.B.Day et al., Phys.Rev.118(1960)864
H.Poth, CERN-EP/86-105
31 - J.Mahalanabis et al., CERN-TH/87-4833,In press in Nucl.Phys.A(1988)
32 - I.L.Grach et al., ITEP, N210(1987)Moscow
33 - R.Bizzarri, CERN 72-10(1972)
34 - D.V.Bugg et al.,Phys.Lett.B194(1987)563
C.B.Dover and J.M.Richard,Ann.Phys.121(1979)70

TABLE CAPTIONS

Tab.1 - Reactions with production of 0,1,2 pions in the $\bar{p}$-nucleon annihilation. πN charge exchange effects are shown separately. In square parantheses the different charge exchange reactions are indicated. a,b indicate reactions with different types of charged particles in the final state. N_T is the total number of charged particles. N_H is the number of heavy particles and $E^{\pm}$ is the equality (=) or the inequality ($\neq$) of the numbers of charged π.

Tab.2 - Features of the charged prongs of the events of type (a) and (b) ; see text. N_H = number of heavy prongs ; $E^{\pm}$ = equality (=) or inequality ($\neq$) of the number of π^- and π^+.

Tab.3 - Observed events of type (a) and (b) and related multiplicity distributions n_c=charged prong multiplicity; n_{π^-}=negative pion multiplicity; N=number of events of type (a) or (b) or (a)+(b); P_i=charged prong multiplicity distributions; (a)%=normalized percentages of events of type (a); (b)%=as above for the type (b) ones. The statistical errors on N_b are equal to those on N_a.

Tab.4 - π^- multiplicity distributions for $\bar{p}p$ and $\bar{p}n$ annihilations on ^{3}He (this work), ^{2}H (Refs. 17 (in parenthesis) and 18), and ^{1}H [1] .
$< n_{\pi^-} >$ = mean number of π^- per event.

Tab.5 - R^a and R^a_b values from ^{2}H and ^{3}He nuclei at rest.

Tab.6 - The ratio R^a_S from different $\bar{N}N$ potential modes and from experiments.

FIGURE CAPTIONS

Fig.1 - σ^a_0/σ^a_1 as a function of R^a.

Fig.2 - $\bar{p}p$ and $\bar{p}n$ annihilation cross sections as functions of the $\bar{p}$ momentum. All the data include annihilation into neutrals (see text).

$\bar{p}p$ annihilation :

(□) Chaloupka et al. [2]

(●) Brueckner et. al. [8]

(—) Brando et. al. [6]. The line with arrows is an extrapolation to values of the $\bar{p}$ momentum lower than those of the experiment.

(···) Sai et al. [5]

(- -) Lowenstein et al. [4]

(·-) Brueckner et al. [7]

$\bar{p}n$ annihilation :

(-·-) Armstrong et al. [13]. Only the statistical error on the negative side is indicated, for the sake of simplicity. The systematic error is similar to the statistical one.

Fig.3 - Cross sections for $\bar{p}p$ -> neutrals and for $\bar{p}p$ ->$\bar{n}n$ charge exchange.

(□) Amaldi et al. [1]

(●) Chaloupka et al. [2]

(○) Hamilton et al. [10]

The lines are guides for the eyes.

Fig.4 - Behaviour of R^a_b as a function of the $\bar{p}$ momentum.

(□) $\bar{p}$ ^{2}H, Bizzarri et al. [17]

(○) $\bar{p}$ ^{2}H, Kalogeropoulos et al. [18]

(▲) $\bar{p}$ ^{4}He, Balestra et al. [19,20]

(▽) $\bar{p}$ ^{3}He, this work

	Set	N_T	N_H	$E\pm$
$\bar{p}^3He$ -->				
$(\bar{p}\,p)$ ------> $p + n + M\pi^0$	a	1	1	=
[$\pi^0n \to \pi^-p$] -> $2p + \pi^- + M\pi^0$	b	3	2	≠
[$\pi^0p \to \pi^+n$] -> $2n + \pi^+ + M\pi^0$	a	1	0	≠
$(\bar{p}\,n)$ -------> $2p + \pi^- + M\pi^0$	b	3	2	≠
[$\pi^0p \to \pi^+n$] -> $p + n + \pi^+ + \pi^- + M\pi^0$	a	3	1	=
[$\pi^-p \to \pi^0n$] -> $n + p + M\pi^0$	a	1	1	=
$(\bar{p}\,p)$ --------> $p + n + \pi^+ + \pi^- + M\pi^0$	a	3	1	=
[$\pi^0p \to \pi^+n$] -> $2n + 2\pi^+ + \pi^- + M\pi^0$	a	3	0	≠
[$\pi^-p \to \pi^0n$] -> $2n + \pi^+ + M\pi^0$	a	1	0	≠
[$\pi^0n \to \pi^-p$] -> $2p + \pi^+ + 2\pi^- + M\pi^0$	b	5	2	≠
[$\pi^+n \to \pi^0p$] -> $2p + \pi^- + M\pi^0$	b	3	2	≠

Tab.1

	N_H	$E^{\pm}$
(a) events	0	$\neq$
	1	=
(b) events	2	$\neq$

Tab.2

n_c	n_{π^-}	N_a	N_b	N_{a+b}	P_i	(a)%	(b)%
1	0	99	_	99	4.90±0.48	4.90±0.48	_
3	1	399±5.20	29	428	39.26±1.09	36.60±1.12	2.66±0.48
5	2	288±8.55	98	386	48.56±1.11	36.23±1.36	12.33±1.11
7	3	22±3.42	25	47	7.13±0.57	3.34±0.58	3.79±0.60
9	4	_	2	2	0.15±0.09	_	0.15±0.09
Totali:				962	100.	81.07±1.92	18.93±1.35

Tab.3

n_{π^-}	^{3}He at rest	^{2}H < 270 MeV/c (<300 MeV/c)	^{1}H 329 MeV/c
$\bar{p}$ p annihilation			
0	6.04±0.59	6.4 ±0.4 (5.6)	6.27±0.53
1	45.15±1.38	42.3 ±1.0 (43.2 ±1.4)	42.38±3.27
2	44.69±1.68	46.9 ±1.1 (47.2±1.8)	47.32±2.82
3	4.12±0.71	4.4±0.3 (4.0±0.7)	4.02±0.64
$<n_{\pi^-}>$	1.469±0.042	1.493±0.017	1.491±0.064
$\bar{p}$ n annihilation			
1	14.05±2.53	16.8±0.8 (15.21±1.1)	
2	65.14±5.86	59.5±1.4 (58.2±2.2)	
3	20.02±3.17	23.0±0.9 (26.6±1.6)	
4	0.79±0.47	0.7±0.2 (0.)	
$<n_{\pi^-}>$	2.075±0.154	2.076±0.040	

Tab.4

R^a and R^a_b values	σ^a_1/σ^a_0	Refs.
R^a_b (d) = 0.75 ± 0.02	0.60± 0.03	[18]
R^a_b (d) = 0.81 ±0.03	0.70± 0.04	[17]
$R^a_b(^3He)$ = 0.47 ±0.04	0.31± 0.03	[this work]
R^a (^3He) = 0.35 ±0.07	0.21± 0.05	[16]
$R^a_b(^4He)$ = 0.48 ±0.03	0.31± 0.03	[20]
R^a (^4He) = 0.48 ±0.1	0.31± 0.08	[16]

Tab.5

Model	R^a	Ref.
Ueda 1	1.	23
Ueda 2	0.742	23
Ueda BST	0.834	23
Bryan-Phillips (static)	0.85	24
Bryan-Phillips (non-static)	0.99	24
Dover-Richard	0.84	25
Paris	1.14	26
Experiment		
($\bar{p}$ p atoms and AGS 795 data)	1.18$\pm$0.14	27
($\bar{N}$ p scattering and $\bar{p}$ p atoms)	0.714	31

Tab.6

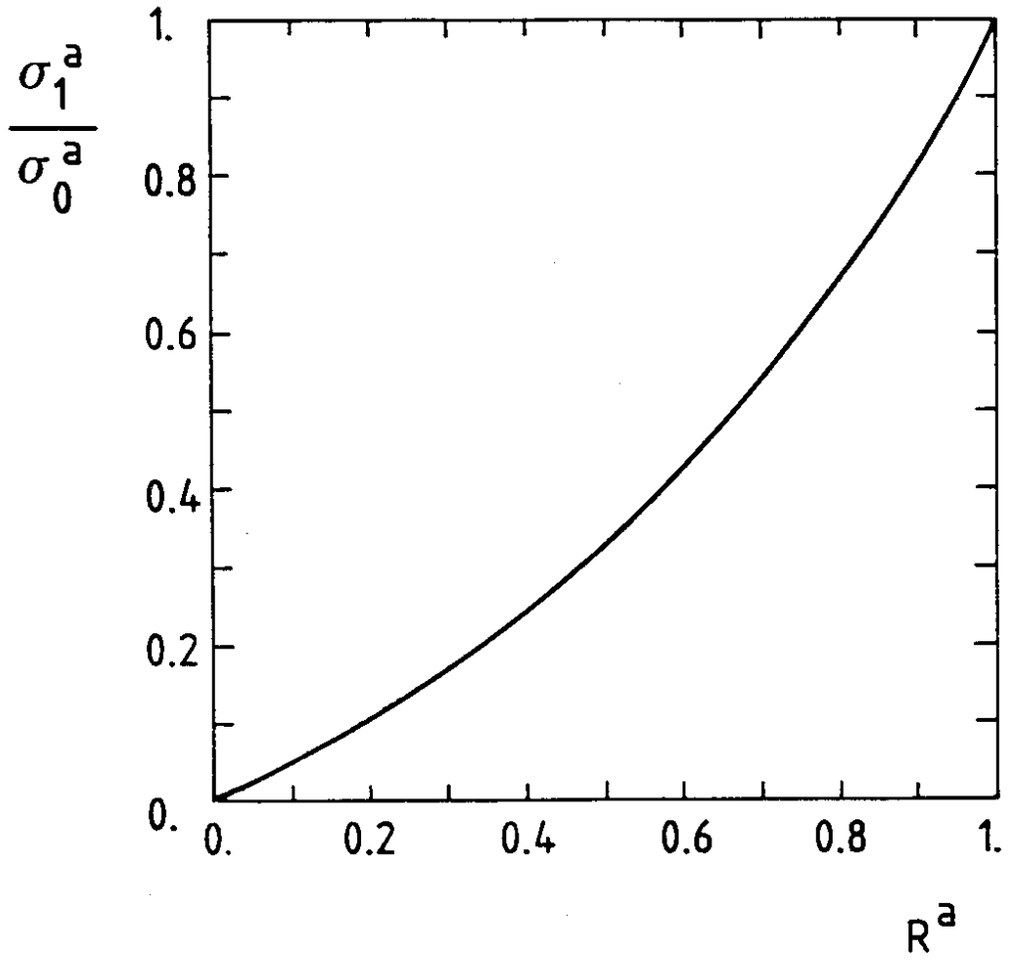

Fig. 1

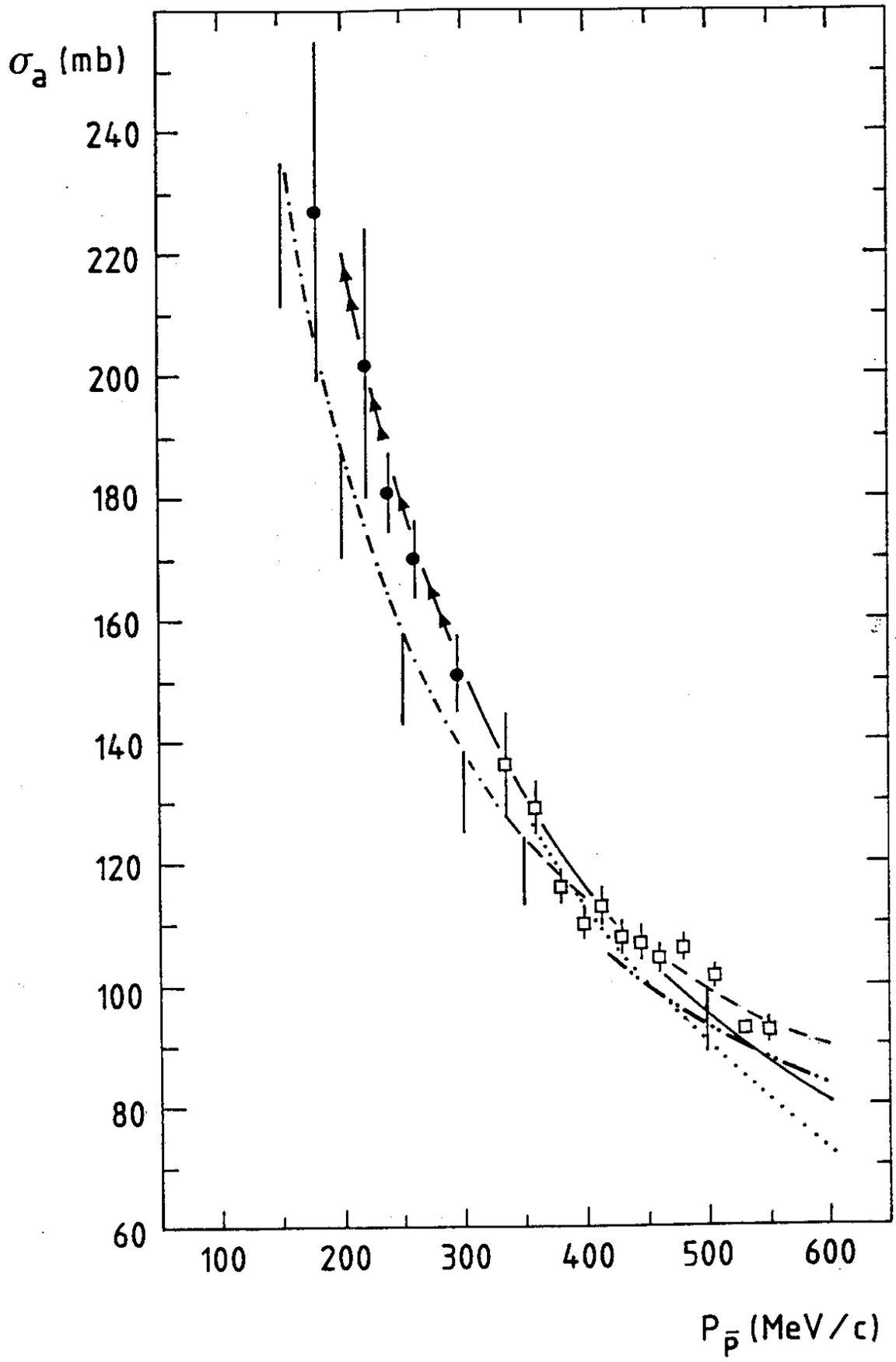
σ_a (mb)
240
220
200
180
160
140
120
100
80
60
100
200
300
400
500
600
$P_{\bar{p}}$ (MeV/c)

Fig. 2

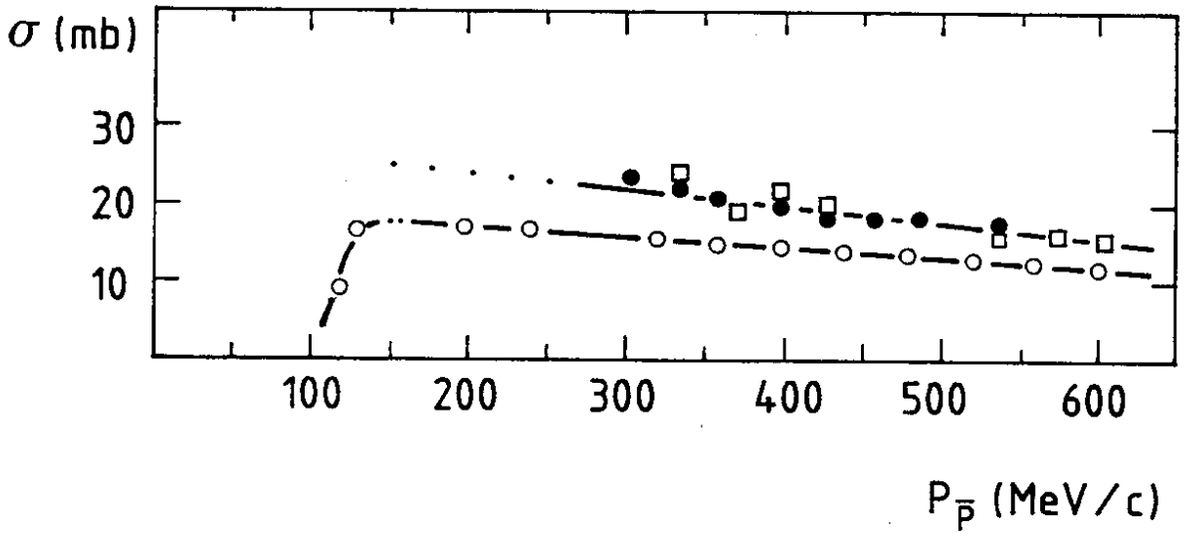

Fig. 3

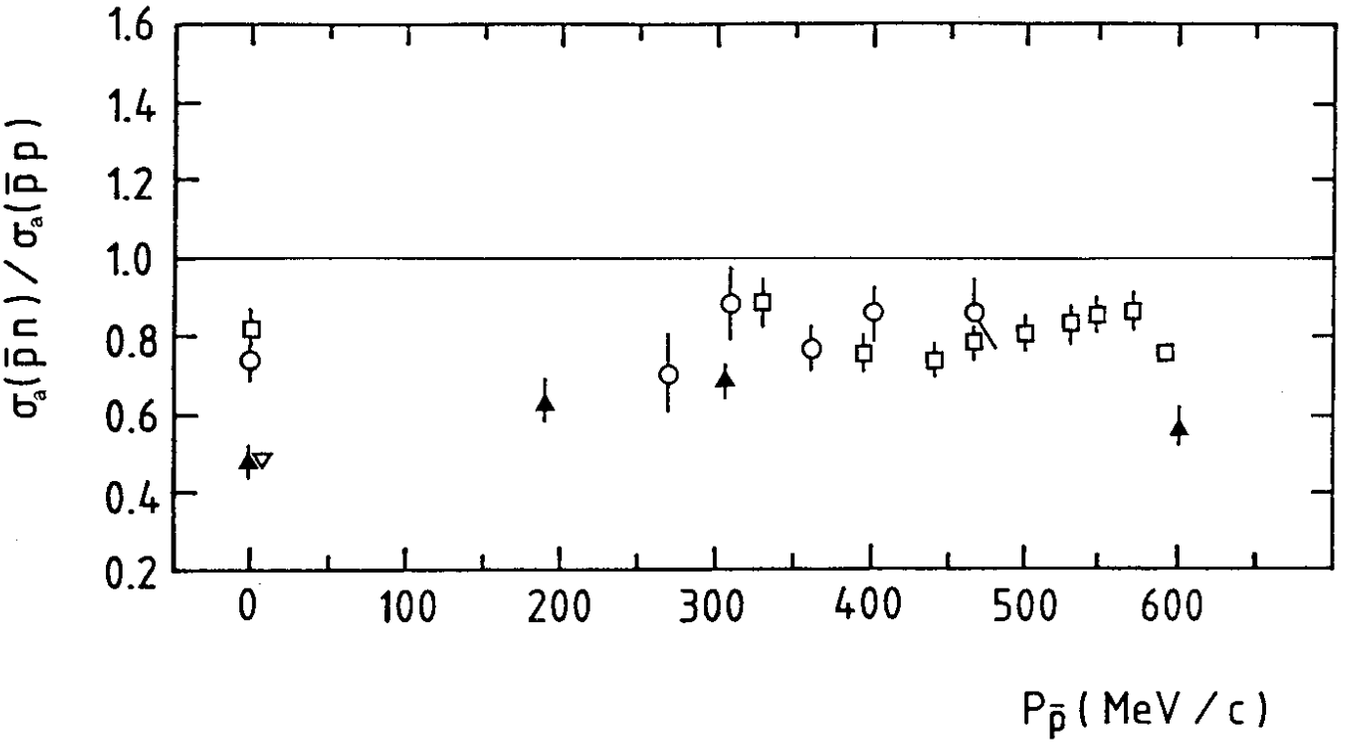
1.6
1.4
1.2
1.0
0.8
0.6
0.4
0.2
0
100
200
300
400
500
600
$\sigma_a(\bar{p}n) / \sigma_a(\bar{p}p)$
$P_{\bar{p}}$ (MeV / c)

Fig. 4